Received: 16 March 2022 | Revised: 7 June 2022 | Accepted: 23 July 2022

DOI: 10.1002/mp.15900

TECHNICAL NOTE

MEDICAL PHYSICS

Technical Note: *rtdsm*—An open-source software for radiotherapy dose-surface map generation and analysis

Haley M. Patrick[1,2] | **John Kildea**[1,2]

[1]Medical Physics Unit, McGill University, Montreal, Quebec, Canada

[2]Cancer Research Program, Research Institute of the McGill University Health Centre, Montreal, Quebec, Canada

Correspondence
Haley M. Patrick, DS1.7141, 1001 boul. Décarie (MUHC); Montréal, QC H4A 3J1, Canada.
Email: haley.patrick@mail.mcgill.ca

Funding information
Natural Sciences and Engineering Research Council of Canada - CREATE program in Responsible Health and Healthcare Data Science; Fonds de Recherche du Québec - Santé; Canada Foundation for Innovation - John R. Evans Leaders Fund

Abstract

Background: Dose-outcome studies in radiation oncology have historically excluded spatial information due to dose-volume histograms being the most dominant source of dosimetric information. In recent years, dose-surface maps (DSMs) have become increasingly popular for characterization of spatial dose distributions and identification of radiosensitive subregions for hollow organs. However, methodological variations and lack of open-source, publicly offered code-sharing between research groups have limited reproducibility and wider adoption.

Purpose: This paper presents *rtdsm*, an open-source software for DSM calculation with the intent to improve the reproducibility of and the access to DSM-based research in medical physics and radiation oncology.

Methods: A literature review was conducted to identify essential functionalities and prevailing calculation approaches to guide development. The described software has been designed to calculate DSMs from DICOM data with a high degree of user customizability and to facilitate DSM feature analysis. Core functionalities include DSM calculation, equivalent dose conversions, common DSM feature extraction, and simple DSM accumulation.

Results: A number of use cases were used to qualitatively and quantitatively demonstrate the use and usefulness of *rtdsm*. Specifically, two DSM slicing methods, planar and noncoplanar, were implemented and tested, and the effects of method choice on output DSMs were demonstrated. An example comparison of DSMs from two different treatments was used to highlight the use cases of various built-in analysis functions for equivalent dose conversion and DSM feature extraction.

Conclusions: We developed and implemented *rtdsm* as a standalone software that provides all essential functionalities required to perform a DSM-based study. It has been made freely accessible under an open-source license on Github to encourage collaboration and community use.

KEYWORDS
dose-surface map, dose-volume analysis, organ unwrapping

1 | INTRODUCTION

Achieving balance between sufficient tumor irradiation and normal tissue sparing is a longstanding challenge in the field of radiotherapy. For this reason, dosimetric constraints for organs at risk (OARs) derived from dose-volume histograms (DVHs) have been an essential component of treatment planning since their introduction in the 1990s.[1] However, DVHs are limited by their lack of spatial information and by the inherent assumption that OARs respond homogeneously to radiation.[2] This assumption is counter to evidence supporting regional variations in OAR sensitivity, which have been reported for multiple organs such as salivary glands, bladder, rectum, and lung[3–7] using a variety of techniques to study spatial dose information.[8]

A popular instrument used to help identify radiosensitive subregions in hollow organs is the dose-surface map (DSM), which projects a region of interest's (ROI) surface dose onto a 2D grid. This is typically achieved by sampling the surface dose across multiple slices of the ROI and cutting and unwrapping its hollow structure to create the map, though some alternative surface dose sampling methods exist.[9,10] To date, DSMs have been used to identify spatial dose features predictive of toxicities for the rectum, bladder, vagina, and heart.[11–15]

Despite their growing popularity, there is a lack of consensus about how to generate DSMs. Most notable is the ways in which the ROI slices are defined: Some groups opt to use axial slices parallel to the slices of the treatment planning image[6,16,17] (planar slicing), while others define them orthogonal to the ROI's central-axis path (CAP)[12,18,19] (noncoplanar slicing), arguing that this better represents ROIs with irregular curvatures. Sampling resolutions and unwrapping approaches can also be disparate. For example, reported rectum DSM resolutions vary from 21×21[6] to 120×200[20] pixels with minimal justification as to why. This issue is further compounded by inconsistent methodological reporting, as not all groups provide sufficient information on their sampling or unwrapping approaches for their work to be reproducible. The lack of consensus, paired with a lack of code and data sharing within the broader community makes it challenging to replicate and validate earlier findings.

In this work, we present a technical description of a new open-source software package that we have developed for DSM calculations called *rtdsm*. To the best of our knowledge, our package is the first open-source DSM software that is highly customizable and capable of implementing both slicing methods, as well providing functionalities for dose accumulation, equivalent dose conversions, and DSM feature extraction. As such, we believe it offers the potential to reduce software development barriers for DSM implementation and provides a referenceable calculation framework to facilitate reproducibility and consistent DSM reporting.

2 | METHODS

2.1 | Planning phase

In order to inform the development of *rtdsm*, we conducted a literature review[21] of the DSM literature and used it to guide our design considerations and identify the needs of the community. The Pubmed and Google Scholar databases were queried using the phrase "'dose surface map*" to identify English language articles published between 2000 and 2021. The references sections of relevant identified articles were also used to identify further relevant papers. Only papers that included a description of the DSM calculation process were included in the final list, which consisted of 30 publications.[5,6,9–20,22–37] The contents of each paper were read in detail to identify the methodology and parameters used for DSM calculation, and if the authors had made their code publicly available. This was followed by a search for dose-surface mapping software packages using the Google search engine and on the GitHub and pypi online code repositories. An overview of the review's findings is presented in Table S1.

TABLE 1 Python library dependencies of *rtdsm*

Library	Usage
pyvista [44]	Create and operate on 3D mesh objects
pydicom [45]	Read DICOM formatted data files
scikit-image [46]	Mesh generation, cluster analysis
scipy [47]	Interpolation operations

Our review found just a single open-source package for noncoplanar DSM calculation (which was not mentioned in its associated journal article)[19] and nothing for planar DSMs. Furthermore, the code bases described in the literature were each restricted to single slicing approaches,[6,18,19] limiting calculation flexibility. Based on these limitations and the commonalities in the calculation and analysis methodologies identified during the review, we determined that *rtdsm* must

1. be open-source to help reduce software development barriers and facilitate standards;
2. support planar and noncoplanar slicing methods to facilitate the most appropriate DSM calculation strategy for each ROI;
3. permit customizable slicing and sampling resolutions to allow for reproduction of previous and future studies;
4. calculate and report common DSM features for use in clinical decision making and dose-outcomes research; and
5. be modularly designed to enable easy implementation of alternative or improved calculation methods in the future.

We opted not to use the existing open-source package of Witztum et al. (2016, https://github.com/bgeorge0/dsm),[19] which provides functionality solely for noncoplanar DSM calculations as it is written for the Matlab platform (The MathWorks, Inc., Natick, MA), and we desired a solution for both slicing methods and DSM analysis that would be fully accessible to the community with minimal cost overhead. After considering the various programming language options available, we selected Python for *rtdsm* due to its popularity, variety of libraries, and open-source nature. The Python libraries utilized by *rtdsm* are listed in Table 1. The software is designed to be imported and used like other python packages, and is available

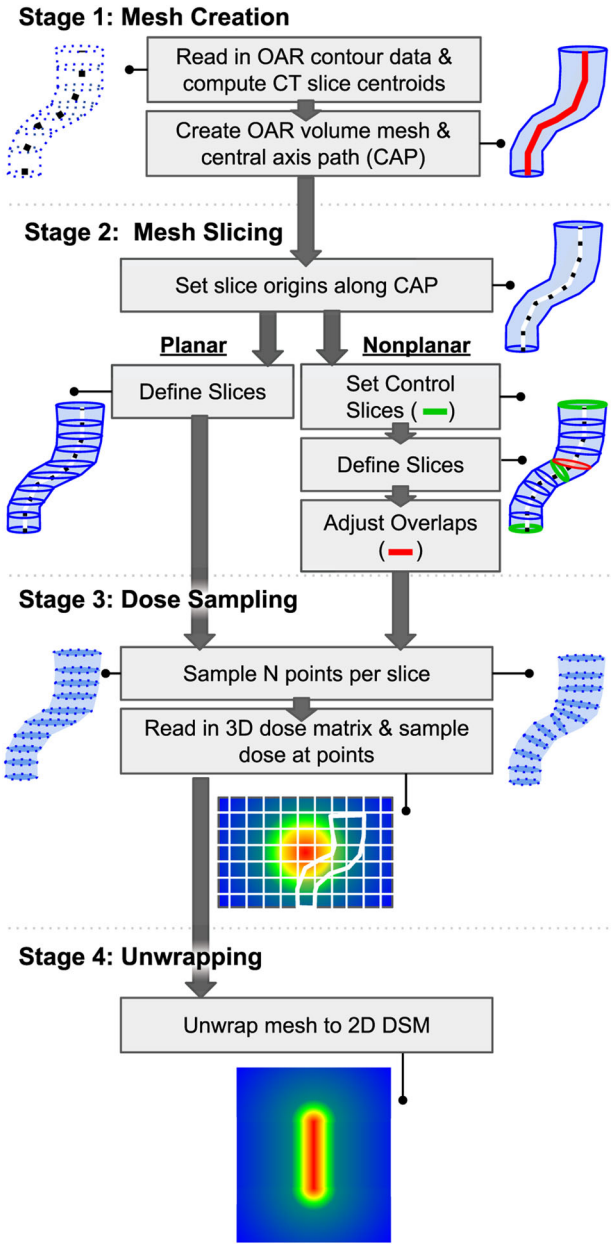

FIGURE 1 The four key stages of a typical dose-surface map generation workflow for an organ at risk, as identified in our literature review and implemented in *rtdsm*

on GitHub (https://github.com/McGillMedPhys/rtdsm). Detailed documentation and tutorials on software implementation are included with the repository in accordance with Python code style standards. The remainder of the section therefore focuses on describing the process used by *rtdsm* to calculate a DSM following the four key stages identified in the literature (Figure 1).

2.2 | Stage 1: Mesh creation

ROI contour information is provided by way of a point-cloud stored in RTStructureSet DICOM-RT format that is generated by the treatment planning system. Once read into *rtdsm*, a surface mesh of the ROI is generated from its point-cloud using a smoothed marching cubes algorithm.[38] While we also tested Delaunay triangulation,[39] we found that it was too sensitive to irregular point-cloud resolution and open surfaces and subsequently produced inadequate meshes for commonly studied ROIs.

In addition to generating the surface mesh, the point-cloud read-in process also calculates the geometric CAP of the ROI using the centroids of the CT slices delineated in the RTStructure file. Alternative user-created CAPs can also be swapped in to replace the default geometric CAP.

2.3 | Stage 2: Mesh slicing

A series of slice origins are specified along the length of the CAP based on the preferred slicing method for the DSM (planar or noncoplanar) and the preferred mapping along the vertical axis. Both 1:1 (where slices are spaced by a constant absolute distance) and scaled mapping (where the number of slices remains constant and spacing adjusts accordingly) can be used to define slice origins in *rtdsm*. As described below, slice planes are then defined at each slice origin according to the chosen slicing method and the centroid of each mesh slice is approximated using the method shown in Figure 2a. This approximated slice centroid is used as the starting point for equiangular ray-casting of a user-defined number of rays. The intersection points of the rays with the surface mesh are then stored in a Python dictionary and used in Stage 3 to sample the dose (dose sampling points).

2.3.1 | Planar slicing

Planar slicing is conducted by defining equally spaced parallel slice planes along a single linear axis of the ROI,[6,16,24] the orientations of which are set using a user-specified slice normal vector. If a user-specified slice normal is not provided, *rtdsm* creates axial planes by default.

2.3.2 | Noncoplanar slicing

Unlike planar slicing, noncoplanar slicing uses slice planes that are each individually orthogonal to the ROI's CAP. Each of these slice planes are defined by a tangent vector to the CAP at the slice origin point, which is determined using the preceding and succeeding points and the CAP's gradient (Figure 2b). Because of these slice planes, the noncoplanar slices may overlap with one another, requiring additional steps for overlap detection

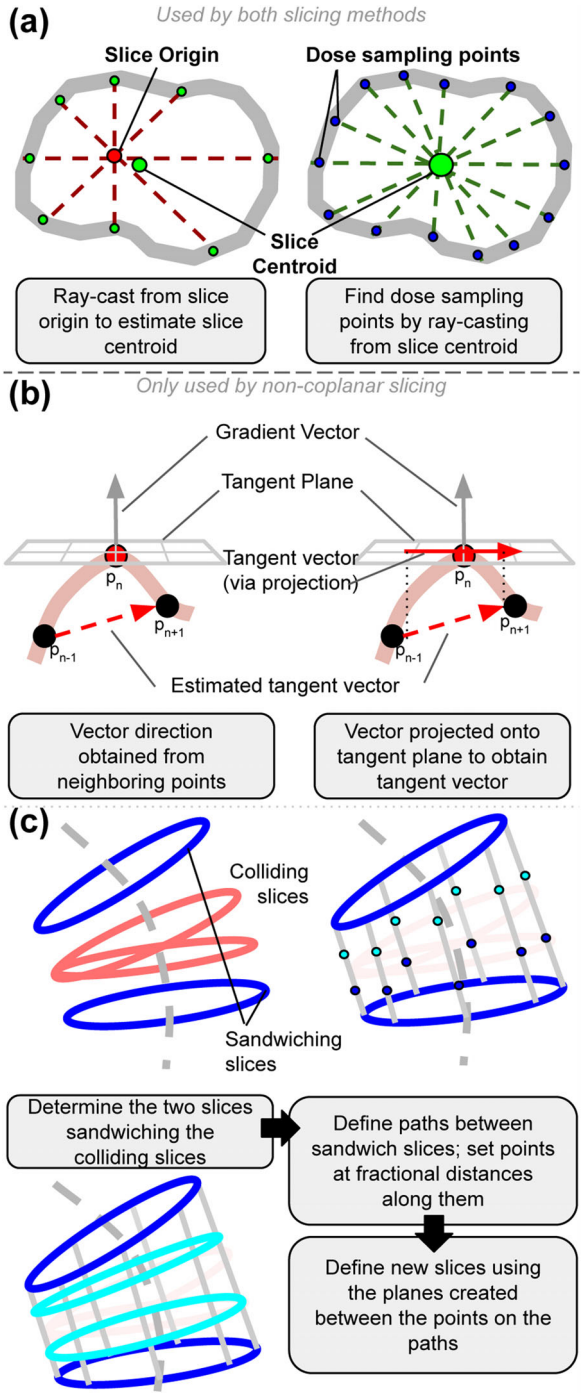

FIGURE 2 Visual explanations of specific operations performed during planar and noncoplanar mesh slicing. (a) Two-step ray-casting approach to acquire dose sampling points used by both slicing methods. (b) Calculation of CAP tangent vectors to define planes for noncoplanar slicing. (c) Correction method to resolve overlapping noncoplanar slices

and correction. To facilitate these additional steps, our implementation of noncoplanar slicing begins by defining "control slices" along the CAP. A control slice is a slice at the start, end, or a point of direction change along the CAP where overlapping slices are more common. They serve to quickly identify slice planes that are angled such that they exit the mesh or overlap many other slice planes, thereby simplifying the level of slice corrections needed. Once the control slices are created, the code checks the proposed slices in ascending order for overlaps with the closest control slices and the preceding neighboring slice. If no overlap is found, the proposed slice is retained, otherwise it is flagged for adjustment. This approach, paired with the selected slice adjustment methodology, removes the need to iteratively check all slices for collisions.

Slice adjustments are performed following the methodology of Witztum et.[19] To briefly summarize, adjacent flagged slices are grouped together with the two nonflagged slices that sandwich them (Figure 2c). Matching angular vertices of the sandwiching slices are connected with one another and the connecting lines are segmented at N equidistant points, where N is equal to the number of flagged slices between them. Corresponding segmentation points are then used to define new nonoverlapping sampling planes for the flagged slices, and ray-casting of the dose sampling points proceeds as normal.

2.4 | Stages 3 and 4: Dose sampling and unwrapping

As is the case for contour data input, *rtdsm* accepts DICOM-RT files with dose information. Dose matrices are read in from RTDose files and are used to sample the dose by means of linear interpolation at the dose sampling points identified during mesh slicing. The cutting open and unwrapping of the DSM is straightforward due to the way in which *rtdsm* defines dose sampling points. This is because the ray-casting process defines rays in clockwise order using a slice-specific orthonormal basis, wherein the j axis (along which the first ray is cast) is always defined to point to the ROI's posterior wall, regardless of slice orientation. If needed, postprocessing can be performed on the output DSM to change the cutpoint.

2.5 | Postprocessing functionalities

Cluster and ellipse-based spatial dose features are calculated by finding the largest contiguous cluster of DSM pixels above a given dose level and fitting an ellipse to them.[6,16,20,32] Table 2 outlines the features developed by Buettner et al. and Moulton et al. that *rtdsm* supports. Additionally, we included support for equivalent dose (EQD) conversion[40] and DSM aggregation (addition, subtraction, and averaging) to facilitate common analysis and visualization strategies.

TABLE 2 Spatial dose features supported by *rtdsm*

Feature	Definition
Cluster Area [6]	The percent area of the DSM covered by the cluster
Cluster Centroid [16]	The center of mass of the cluster. Provided in units of array indices and percent of the lateral and longitudinal spans
Cluster Lateral Extent [16]	The percent of the lateral span of the DSM covered by the cluster
Cluster Longitudinal Extent [16]	The percent of the longitudinal span of the DSM covered by the cluster
Ellipse Area [16]	The percent area of the DSM covered by the ellipse
Ellipse Angle [16]	The rotation of the ellipse, in radians
Ellipse Eccentricity [6]	The eccentricity of the ellipse
Ellipse Lateral Extent [6]	The percent of the lateral span of the DSM covered by a projection of the ellipse's lateral axis onto the DSM's lateral axis
Ellipse Longitudinal Extent [6]	The percent of the longitudinal span of the DSM covered by a projection of the ellipse's longitudinal axis onto the DSM's longitudinal axis

3 | RESULTS

3.1 | DSMs

The performance and capabilities of *rtdsm* were tested using using retrospective data from 36.25 Gy in 5 fraction VMAT plans created in Eclipse (Varian Medical Systems, Palo Alto, CA). Forty planar and noncoplanar rectum DSMs were calculated using 3 mm stepsize 1:1 vertical mapping, with 45 points per slice. On average, calculation of the planar DSMs took 2.8 min ($\approx$ 4.2 s/DSM) and 5.7 min ($\approx$ 8.5 s/DSM) for noncoplanar on an Intel® Xeon® CPU X3440 (2.53 GHz) with 4 GB of RAM. Figure 3 shows the rectum DSMs obtained for several patients and illustrates how rectum shape and slicing choice influence the final DSM. For ROIs with CAPs that closely follow the longitudinal axis of the contoured image, the planar and noncoplanar slices are similar, resulting in similar DSMs. However, if the CAP significantly traverses anteriorly–posteriorly or left–right, the slices and subsequent DSMs are quite different. As seen in Figure 3, the orientation of planar slices in these example cases leads to the inclusion of more anterior points that lie in the high-dose region, increasing the size of the hotspot relative to the noncoplanar DSM.

3.2 | DSM conversions and combinations

In many studies, it can be beneficial to combine multiple DSMs in order to visually compare patient cohorts. *rtdsm*'s DSM combination function provides a built-in method to do this, under the assumption that all DSMs are aligned at the first (inferior-most) slice and use the same vertical sampling approach. As an example of its possible use cases, noncoplanar rectum DSMs were calculated using scaled vertical mapping to produce normalized 30×30 pixel DSMs for two cohorts of 10 prostate cancer patients each, who were either prescribed 60 Gy in 20 fractions (hypofractionated IMRT) or 36.25 Gy in 5 fractions (SBRT). Figure 4 shows the average DSM for each cohort, as well as their difference calculated by *rtdsm*.

In order to properly compare them, the DSMs were converted to EQD2 Gy using *rtdsm*'s built-in conversion function with an α/β ratio of 2.3.[9] Through the comparison it is made apparent that the SBRT treatment regularly delivers doses exceeding 80 Gy to a small anterior region of the rectum (mean area: 4.8%), whereas this is less common for the IMRT treatment (mean area: 0.7%). However, the IMRT treatment delivers doses of $\geq$ 40 Gy to noticeably larger portions of the rectum than SBRT treatment (32.5% vs. 15.7%).

3.3 | Spatial features

A quantitative comparison of the example cohorts from the previous section was conducted by calculating spatial features for 15, 30, 45, 60, and 75 Gy clusters using the EQD2 Gy converted DSMs (Figure 5). As noted visually, the IMRT treatment (red points) delivered dose to systematically larger areas of the rectum than the SBRT treatment (blue points), which is also apparent from the DVH and the area-based features. However, spatial features also revealed that the investigated dose levels spanned systematically larger longitudinal proportions of the rectum in the IMRT group than the SBRT group for all dose levels, but only for those levels below 60 Gy when examining lateral span. These patterns may be relevant to differences in outcomes between the two groups and are not immediately apparent based on volume or area information alone, thus highlighting the value of the spatial-dose features. Features calculated from planar DSMs are shown in Figure S2 for interested readers.

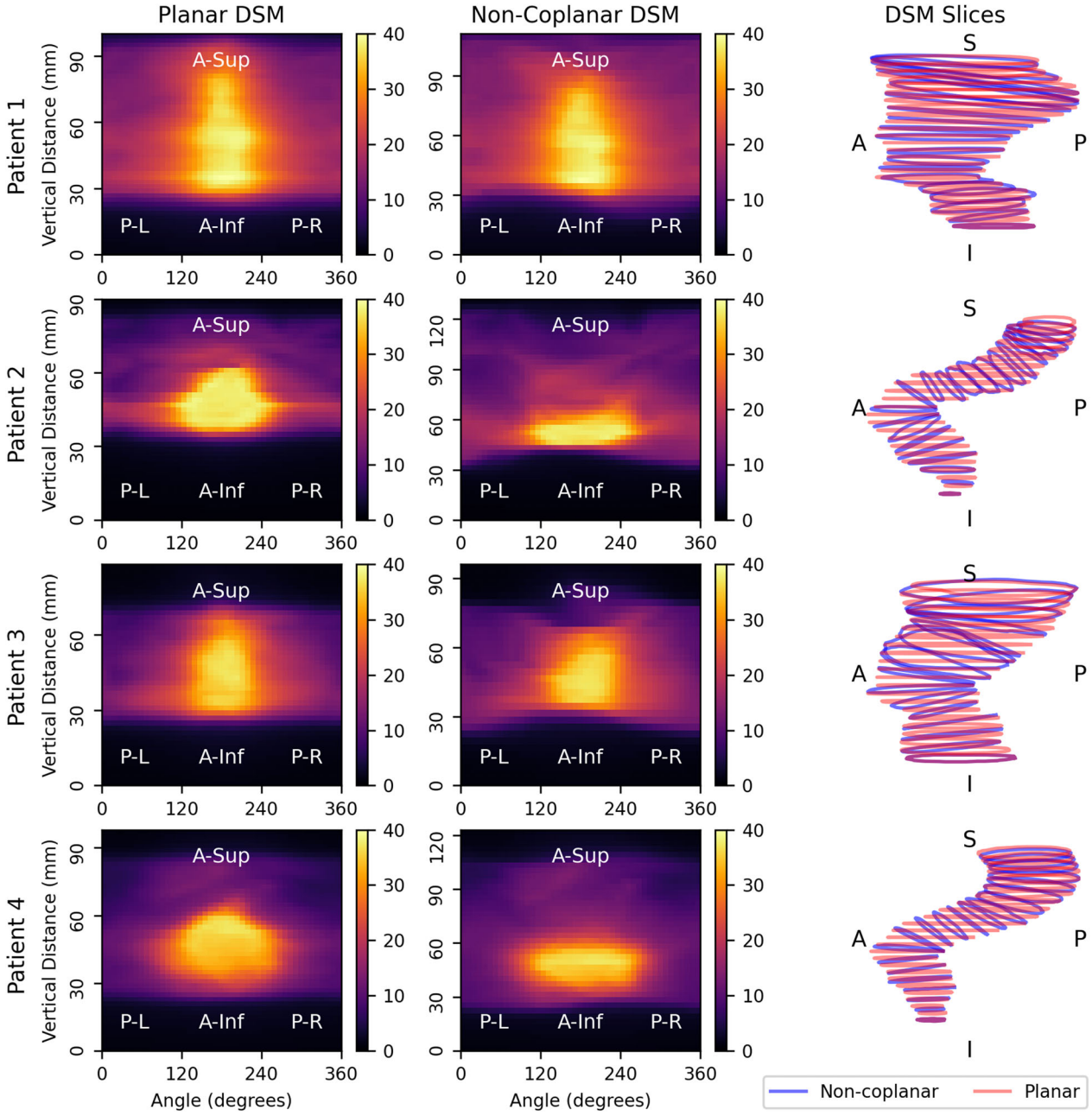

FIGURE 3 Planar DSMs (left), noncoplanar DSMs (center), and the slices of the ROI used to construct the DSMs (right) of four example patients (units: Gy). Individual vertical axes are used for each DSM in order to illustrate how choice of slicing method influences sampling path length and DSM shape. In the right column, planar slices are shown in pale red and noncoplanar slices in dark blue. For clarity, only every second slice is shown.

4 | DISCUSSION

We have presented a technical overview of a new open-source package for DSM calculation that we have developed called *rtdsm*. Using retrospective data, we have demonstrated *rtdsm*'s ability to calculate planar and noncoplanar DSMs, combine and convert cohort data, and extract common spatial-dose features to enable users to perform standard DSM-based studies.

DSMs have been used in dose-outcome research since the early 2000s, but calculation tools have largely remained as custom in-house developments with little exchange between groups. For example, from our reading of the author lists, it appears that most rectal DSM papers using the more complex noncoplanar approach include an author or associate of the original 2004 method paper by Hoogeman et al.[11,12,18,33,34] Nonassociated groups appear to have largely opted to use the simpler-to-develop planar approach, despite noncoplanar DSMs being arguably a more appropriate representation of the rectum structure. *rtdsm* is the first DSM codebase, to our knowledge, to support both

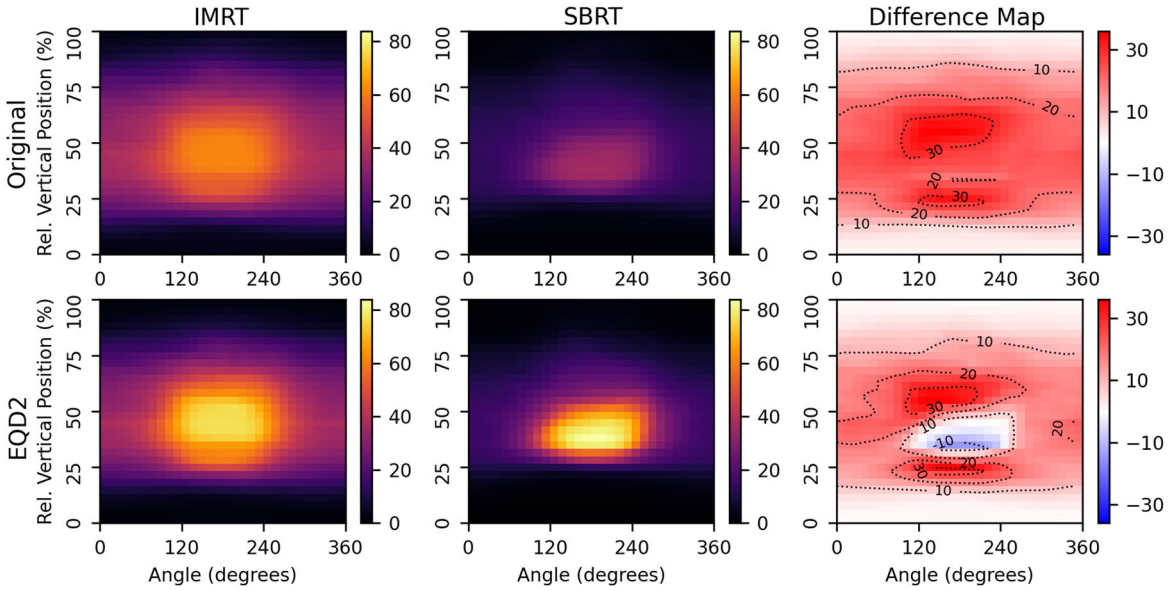

FIGURE 4 Average dose-surface maps for the IMRT and SBRT cohorts (10 patients each), before and after EQD2 Gy conversion, in units of Gy. Difference maps are also shown with contours indicating specific dose thresholds.

calculation methods that is also an open-source release, inline with our goal to remove the large development barrier to the noncoplanar approach and increasing its accessibility to more researchers.

In addition to removing programming barriers, the accessibility of *rtdsm* has the potential to improve DSM reproducibility between groups, which is becoming an area of concern as the methodology gains in popularity. Mylona et al.[35] recently reported poor reproducibility of toxicity-predictive subregions from bladder DSMs of prostate patients when comparing their results to three other studies. Despite similar DSM construction and analysis approaches, it appears variations in vertical mapping methods between groups (scaled mapping by Mylona, 1:1 mapping truncated at 25 or 45 mm by others[5,13 36]) influenced the reproducibility of results. Similar reproducibility issues may also exist for rectal DSMs, especially considering the greater diversity of slicing methods, vertical mapping schemes, and analysis approaches used by different researchers. The result of Mylona's study is an important example of how the results of DSM analyses depend on the calculation methods used and how the lack of methodological standardization over the past two decades may be impeding confirmation of important results. We present *rtdsm* as an accessible open-source package and as an opportunity to begin the discussion around DSM standardization. It is designed to be a software with which research groups can easily test the methods and findings of each other by applying custom settings.

rtdsm is published at github.com and will continue to be updated and built upon as the needs of the DSM field evolve, either by its original developers or by new contributors who are welcome to support the project. For example, we have already identified different CAP-generating approaches, such as the racecar[41] or electric field path[22] methods, as areas for potential future improvement, along with implementation of more advanced unwrapping approaches.[19] Support for additional analysis approaches akin to the significance testing popularized by Chen et al.[42] are other areas of active development. While a potential limitation of the current version *rtdsm* is that testing has largely focused on rectum structures to date, further generalizability tests using other organs are planned. Further investigations into additional uses of *rtdsm* are also of interest, including the creation of surface maps from other 3D medical data like positron emission tomography (PET) or electrocardiography (ECG) images, as well as the extraction of "dosiomic" features from DSMs.[43]

5 | CONCLUSIONS

We have presented a technical overview of *rtdsm*, a new software for the calculation and evaluation of DSMs. *rtdsm* is a python package that works by computing the dose to the surface of a 3D contoured object and unwrapping it to a 2D map according to user specifications. It is highly flexible and extensible with sufficiently small calculation times to facilitate analysis of large data sets. The results presented in this work demonstrate how *rtdsm* can be used to (1) create multiple types of DSMs, (2) calculate DSM features, and (3) evaluate spatial-dose variations between cohorts. *rtdsm* has been made publicly accessible through GitHub (https://github.com/McGillMedPhys/rtdsm) with

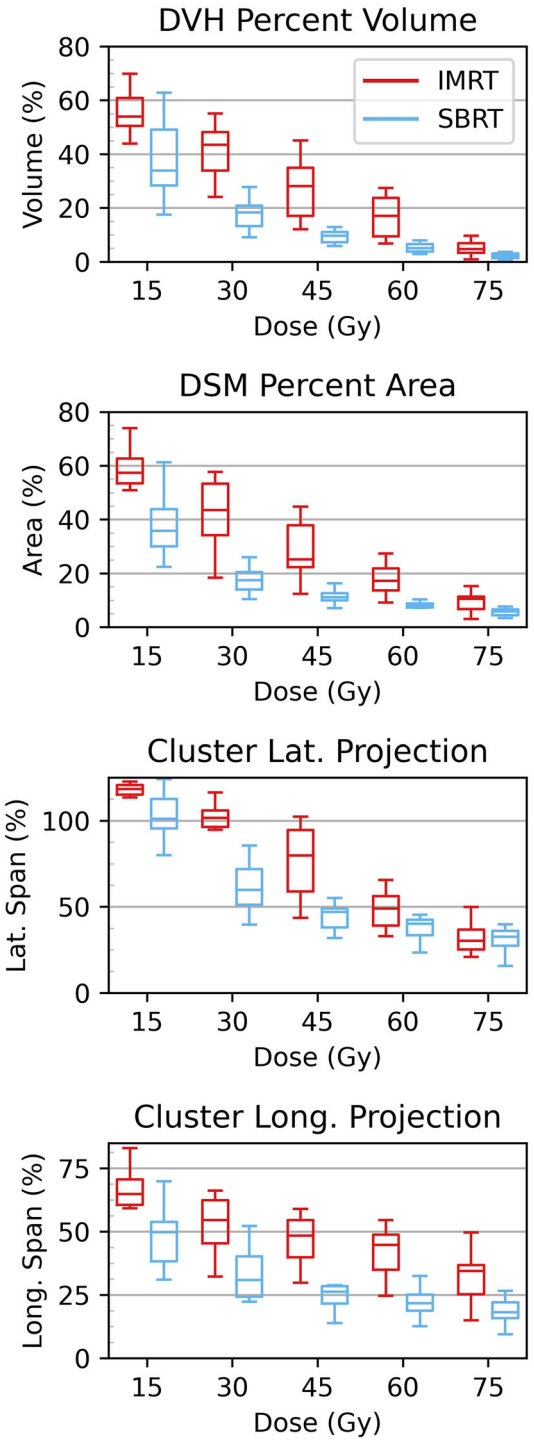

FIGURE 5 Boxplots of the dose features of the IMRT and SBRT cohorts, converted to EQD2 Gy: (a) percent volume (from DVHs), (b) percent area (from DSMs), (c) lateral projection (from DSMs), and (d) longitudinal projection (from DSMs)

detailed examples and documentation and can be freely used or contributed to by any user.

ACKNOWLEDGMENTS

We gratefully appreciate the insights and support of Luc Galarneau for valuable discussions regarding the construction and packaging of *rtdsm*. H.M.P. acknowledges funding from the Fonds de recherche du Québec - Santé in the form of a Doctoral Training Award, as well as partial support by the CREATE Responsible Health and Healthcare Data Science (SDRDS) grant of the Natural Sciences and Engineering Research Council.

CONFLICT OF INTEREST

The authors have declared no conflict of interest.

REFERENCES

1. Emami B, Lyman J, Brown A, et al. Tolerance of normal tissue to therapeutic irradiation. *Int J Radiat Oncol Biol Phys*. 1991;21:109-122.
2. Jaffray DA, Lindsay PE, Brock KK, Deasy JO, Tomé WA. Accurate accumulation of dose for improved understanding of radiation effects in normal tissue. *Int J Radiat Oncol Biol Phys*. 2010;76:S135-139.
3. Jiang W, Lakshminarayanan P, Hui X, et al. Machine learning methods uncover radiomorphologic dose patterns in salivary glands that predict xerostomia in patients with head and neck cancer. *Advances in Radiation Oncology*. 2019;4(2):401-412.
4. Van Luijk P, Pringle S, Deasy JO, et al. Sparing the region of the salivary gland containing stem cells preserves saliva production after radiotherapy for head and neck cancer. *Sci Transl Med*. 2015;7(305):305ra147-305ra147.
5. Palorini F, Cozzarini C, Gianolini S, et al. First application of a pixel-wise analysis on bladder dose-surface maps in prostate cancer radiotherapy. *Radiother Oncol*. 2016;119(1):123-128.
6. Buettner F, Gulliford SL, Webb S, Sydes MR, Dearnaley DP, Partridge M. Assessing correlations between the spatial distribution of the dose to the rectal wall and late rectal toxicity after prostate radiotherapy: an analysis of data from the MRC RT01 trial (ISRCTN 47772397). *Phys Med Biol*. 2009;54(21):6535.
7. Seppenwoolde Y, De Jaeger K, Boersma LJ, Belderbos JSA, Lebesque JV. Regional differences in lung radiosensitivity after radiotherapy for non-small-cell lung cancer. *Int J Radiat Oncol Biol Phys*. 2004;60(3):748-758.
8. Ebert MA, Gulliford S, Acosta O, et al. Spatial descriptions of radiotherapy dose: normal tissue complication models and statistical associations. *Phys Med Biol*. 2021;66(12):12TR01.
9. Shelley LEA, Sutcliffe MPF, Thomas SJ, et al. Associations between voxel-level accumulated dose and rectal toxicity in prostate radiotherapy. *Phys Imaging Radiat Oncol*. 2020;14:87-94.
10. Munbodh R, Jackson A, Bauer J, Ross SC, Zelefsky MJ. Dosimetric and anatomic indicators of late rectal toxicity after high-dose intensity modulated radiation therapy for prostate cancer. *Med Phys*. 2008;35(5):2137-2150.
11. Heemsbergen WD, Hoogeman MS, Hart GAM, Lebesque JV, Koper PCM. Gastrointestinal toxicity and its relation to dose distributions in the anorectal region of prostate cancer patients treated with radiotherapy. *Int J Radiat Oncol Biol Phys*. 2005;61(4):1011-1018.
12. Wortel RC, Witte MG, Heide UA, et al. Dose-surface maps identifying local dose-effects for acute gastrointestinal toxicity after radiotherapy for prostate cancer. *Radiother Oncol*. 2015;117(3):515-520.
13. Yahya N, Ebert MA, House MJ, et al. Modeling urinary dysfunction after external beam radiation therapy of the prostate using bladder dose-surface maps: evidence of spatially variable response of the bladder surface. *Int J Radiat Oncol Biol Phys*. 2017;97(2):420-426.
14. Serban M, Leeuw AAC, Tanderup K, Jürgenliemk-Schulz IM. Vaginal dose-surface maps in cervical cancer brachytherapy: methodology and preliminary results on correlation with morbidity. *Brachytherapy*. 2021;20(3):565-575.

15. McWilliam A, Dootson C, Graham L, Banfill K, Abravan A, Herk M. Dose surface maps of the heart can identify regions associated with worse survival for lung cancer patients treated with radiotherapy. *Phys Imaging Radiat Oncol*. 2020;15:46-51.
16. Moulton CR, House MJ, Lye V, et al. Spatial features of dose-surface maps from deformably-registered plans correlate with late gastrointestinal complications. *Phys Med Biol*. 2017;62(10):4118.
17. Chen J, Chen H, Zhong Z, et al. Investigating rectal toxicity associated dosimetric features with deformable accumulated rectal surface dose maps for cervical cancer radiotherapy. *Radiat Oncol*. 2018;13(1):1-10.
18. Hoogeman MS, Van Herk M, De Bois J, Muller-Timmermans P, Koper PCM, Lebesque JV. Quantification of local rectal wall displacements by virtual rectum unfolding. *Radiother Oncol*. 2004;70:21-30.
19. Witztum A, George B, Warren S, Partridge M, Hawkins MA. Unwrapping 3D complex hollow organs for spatial dose surface analysis. *Med Phys*. 2016;43(11):6009-6016.
20. Onjukka E, Fiorino C, Cicchetti A, et al. Patterns in ano-rectal dose maps and the risk of late toxicity after prostate IMRT. *Acta Oncologica*. 2019;58(12):1757-1764.
21. Grant MJ, Booth A. A typology of reviews: an analysis of 14 review types and associated methodologies: a typology of reviews, Maria J. Grant & Andrew Booth. *Health Info Libr J*. 2009;26(2):91-108.
22. Wang G, McFarland EG, Brown BP, Vannier MW. GI tract unraveling with curved cross sections. *IEEE Trans Med Imaging*. 1998;2434:307-315.
23. Meijer GJ, Van Den Brink M, Hoogeman MS, Meinders J, Lebesque JV. Dose-wall histograms and normalized dose-surface histograms for the rectum: a new method to analyze the dose distribution over the rectum in conformal radiotherapy. *Int J Radiat Oncol Biol Phys*. 1999;45(4):1073-1080.
24. Tucker SL, Zhang M, Dong L, Mohan R, Kuban D, Thames HD. Cluster model analysis of late rectal bleeding after IMRT of prostate cancer: a case-control study. *Int J Radiat Oncol Biol Phys*. 2006;64(4):1255-1264.
25. Lin ENJT, Kristinsson J, Philippens MEP, et al. Reduced late rectal mucosal changes after prostate three-dimensional conformal radiotherapy with endorectal balloon as observed in repeated endoscopy. *Int J Radiat Oncol Biol Phys*. 2007;67(3):799-811.
26. Buettner F, Gulliford SL, Webb S, Partridge M. Using dose-surface maps to predict radiation-induced rectal bleeding: a neural network approach. *Phys Med Biol*. 2009;57(17):5139.
27. Buettner F, Gulliford SL, Webb S, Partridge M. Modeling late rectal toxicities based on a parameterized representation of the 3D dose distribution. *Phys Med Biol*. 2011;56(7):2103.
28. Murray J, McQuaid D, Dunlop A, et al. SU-E-J-14: a novel approach to evaluate the dosimetric effect of rectal variation during image guided prostate radiotherapy. *Med Phys*. 2014;41(6part6):157-157.
29. Scaife JE, Thomas SJ, Harrison K, et al. Accumulated dose to the rectum, measured using dose-volume histograms and dose-surface maps, is different from planned dose in all patients treated with radiotherapy for prostate cancer. *Br J Radiol*. 2015;88:20150243.
30. Casares-Magaz O, Muren LP, Moiseenko V, et al. Spatial rectal dose/volume metrics predict patient-reported gastro-intestinal symptoms after radiotherapy for prostate cancer. *Acta Oncol*. 2017;56(11):1507-1513.
31. Shelley LEA, Scaife JE, Romanchikova M, et al. Delivered dose can be a better predictor of rectal toxicity than planned dose in prostate radiotherapy. *Radiother Oncol*. 2017;123(3):466-471.
32. Vanneste BGL, Buettner F, Pinkawa M, Lambin P, Hoffmann AL. Ano-rectal wall dose-surface maps localize the dosimetric benefit of hydrogel rectum spacers in prostate cancer radiotherapy. *Clin Transl Oncol*. 2019;14:17-24.
33. Reijtenbagh DMW, Godart J, Mens JWM, Heijkoop ST, Heemsbergen WD, Hoogeman MS. Patient-reported acute GI symptoms in locally advanced cervical cancer patients correlate with rectal dose. *Radiother Oncol*. 2020;148:38-43.
34. Heemsbergen WD, Incrocci L, Pos FJ, Heijmen BJM, Witte MG. Local dose effects for late gastrointestinal toxicity after hypofractionated and conventionally fractionated modern radiotherapy for prostate cancer in the HYPRO trial. *Front Oncol*. 2020;10:469.
35. Mylona E, Cicchetti A, Rancati T, et al. Local dose analysis to predict acute and late urinary toxicities after prostate cancer radiotherapy: assessment of cohort and method effects. *Radiother Oncol*. 2020;147:40-49.
36. Improta I, Palorini F, Cozzarini C, et al. Bladder spatial-dose descriptors correlate with acute urinary toxicity after radiation therapy for prostate cancer. *Phys Med*. 2016;32(3):506-511.
37. Dankers F, Wijsman R, Troost EGC, Monshouwer R, Bussink J, Hoffmann AL. Esophageal wall dose-surface maps do not improve the predictive performance of a multivariable NTCP model for acute esophageal toxicity in advanced stage NSCLC patients treated with intensity-modulated (chemo-)radiotherapy. *Phys Med Biol*. 2017;62(9):3668.
38. Lewiner T, Lopes H, Vieira AW, Tavares G. Efficient implementation of marching cubes' cases with topological guarantees. *J Graphics Tools*. 2003;8(2):1-15.
39. Baker TJ. Automatic mesh generation for complex three-dimensional regions using a constrained Delaunay triangulation. *Eng Computers: Int J Simulat-Based Eng*. 1989;5(3):161-175.
40. Bentzen SM, Dörr W, Gahbauer R, et al. Bioeffect modeling and equieffective dose concepts in radiation oncology—terminology, quantities and units. *Radiother Oncol*. 2012;105(2):266-268.
41. Ulén J, Strandmark P, Kahl F. Shortest paths with higher-order regularization. *IEEE Trans Pattern Anal Mach Intell*. 2015;37(12):2588-2600.
42. Chen C, Witte M, Heemsbergen W, Herk MV. Multiple comparisons permutation test for image based data mining in radiotherapy. *Radiat Oncol*. 2013;8(1):1-10.
43. Gabryś HS, Buettner F, Sterzing F, Hauswald H, Bangert M. Design and selection of machine learning methods using radiomics and dosiomics for normal tissue complication probability modeling of xerostomia. *Front Oncol*. 2018;8:35.
44. Sullivan C, Kaszynski A. PyVista: 3D plotting and mesh analysis through a streamlined interface for the Visualization Toolkit (VTK). *J Open Source Software*. 2019;4(37):1450.
45. Mason D. SU-E-T-33: Pydicom: an open source DICOM library. 2011;38(6part10):3493-3493.
46. Van Der Walt S, Schönberger JL, Nunez-Iglesias J, et al. Scikit-image: image processing in python. *PeerJ*. 2014;2:e453.
47. Virtanen P, et al. SciPy 1.0: fundamental algorithms for scientific computing in Python. *Nature Methods*. 2020;17(3):261-272.

SUPPORTING INFORMATION

Additional supporting information can be found online in the Supporting Information section at the end of this article.

How to cite this article: Patrick HM, Kildea J. Technical Note: *rtdsm*—An open-source software for radiotherapy dose-surface map generation and analysis. *Med Phys*. 2022;1-9. https://doi.org/10.1002/mp.15900